

Hyperglycemia-Triggered Sphingosine-1-Phosphate and Sphingosine-1-Phosphate Receptor 3 Signaling Worsens Liver Ischemia/Reperfusion Injury by Regulating M1/M2 Polarization

Yuanchang Hu,* Chao Yang,* Gefengqiang Shen,* Shikun Yang, Xuyu Cheng, Feng Cheng, Jianhua Rao, and Xuehao Wang

Hepatobiliary Center, The First Affiliated Hospital of Nanjing Medical University, Key Laboratory of Liver Transplantation, Chinese Academy of Medical Sciences, Nanjing, China

Hyperglycemia aggravates hepatic ischemia/reperfusion injury (IRI), but the underlying mechanism for the aggravation remains elusive. Sphingosine-1-phosphate (S1P) and sphingosine-1-phosphate receptors (S1PRs) have been implicated in metabolic and inflammatory diseases. Here, we discuss whether and how S1P/S1PRs are involved in hyperglycemia-related liver IRI. For our *in vivo* experiment, we enrolled diabetic patients with benign hepatic disease who had liver resection, and we used streptozotocin (STZ)-induced hyperglycemic mice or normal mice to establish a liver IRI model. *In vitro* bone marrow-derived macrophages (BMDMs) were differentiated in high-glucose (HG; 30 mM) or low-glucose (LG; 5 mM) conditions for 7 days. The expression of S1P/S1PRs was analyzed in the liver and BMDMs. We investigated the functional and molecular mechanisms by which S1P/S1PRs may influence hyperglycemia-related liver IRI. S1P levels were higher in liver tissues from patients with diabetes mellitus and mice with STZ-induced diabetes. S1PR3, but not S1PR1 or S1PR2, was activated in liver tissues and Kupffer cells under hyperglycemic conditions. The S1PR3 antagonist CAY10444 attenuated hyperglycemia-related liver IRI based on hepatic biochemistry, histology, and inflammatory responses. Diabetic livers expressed higher levels of M1 markers but lower levels of M2 markers at baseline and after ischemia/reperfusion. Dual-immunofluorescence staining showed that hyperglycemia promoted M1 (CD68/CD86) differentiation and inhibited M2 (CD68/CD206) differentiation. Importantly, CAY10444 reversed hyperglycemia-modulated M1/M2 polarization. HG concentrations *in vitro* also triggered S1P/S1PR3 signaling, promoted M1 polarization, inhibited M2 polarization, and enhanced inflammatory responses compared with LG concentrations in BMDMs. In contrast, S1PR3 knockdown significantly retrieved hyperglycemia-modulated M1/M2 polarization and attenuated inflammation. In conclusion, our study reveals that hyperglycemia specifically triggers S1P/S1PR3 signaling and exacerbates liver IRI by facilitating M1 polarization and inhibiting M2 polarization, which may represent an effective therapeutic strategy for liver IRI in diabetes.

Liver Transplantation 25 1074–1090 2019 AASLD.

Received September 24, 2018; accepted April 4, 2019.

Diabetes mellitus (DM) is a complex and multisystem disease.⁽¹⁾ Both type 1 diabetes (T1D) and type 2 diabetes (T2D) are characterized by hyperglycemia,

which has been shown to trigger chronic inflammation.⁽²⁾ Hyperglycemia is associated with high morbidity and mortality after liver transplantation.^(3–6) The standardized mortality rate from end-stage liver disease is also higher in patients with diabetes compared with those without diabetes.⁽⁷⁾

Liver ischemia/reperfusion injury (IRI) is a major cause of acute postoperative liver dysfunction and failure. In the case of liver transplantation, IRI is associated with a high incidence of acute and chronic

Abbreviations: ALT, alanine aminotransferase; ARG1, arginase 1; AST, aspartate aminotransferase; BMDM, bone marrow-derived macrophage; DAPI, 4',6-diamidino-2-phenylindole; DM, diabetes

rejection.^(8,9) Hyperglycemia can aggravate liver ischemia/reperfusion (IR), but the mechanism remains to be elucidated.⁽¹⁰⁾

Sphingolipid metabolite sphingosine-1-phosphate (S1P) is one of the most important bioactive lysophospholipids. It has been implicated in the development of inflammatory and metabolic diseases.⁽¹¹⁻¹⁵⁾ Altered sphingolipid metabolism occurs in hypoxic and ischemic injury.⁽¹⁶⁾ For example, plasma S1P levels increase during myocardial infarction.⁽¹⁷⁾ S1P1 expressed in proximal tubule cells attenuates kidney IRI.⁽¹⁸⁾ Although activation of sphingosine-1-phosphate receptor (S1PR) 3 protects hearts from IRI, S1PR3^{-/-} mice are protected from kidney and pulmonary IRI compared with wild-type (WT) mice.⁽¹⁹⁻²¹⁾ Therefore, the role of S1P in IRI may be organ specific, perhaps relating to the

subtypes of S1P receptors. There is also strong evidence supporting critical roles of the S1P/S1PR system in the progression of DM, including insulin sensitivity, insulin secretion, and development of a diabetic inflammatory state.⁽²²⁾ However, there is little known about the role and molecular mechanisms of the S1P/S1PR system in hyperglycemia-exacerbated liver IRI.

In this study, we demonstrated that diabetes-associated hyperglycemia has a significantly negative impact on liver IRI and that the hyperglycemia-triggered S1P/S1PR3 pathway worsens liver IRI by regulating M1/M2 polarization, which may represent an effective therapeutic strategy for diabetes-related liver surgery.

Patients and Methods

PATIENTS

Liver tissues were obtained from 15 patients with benign liver disease with DM (type 1 diabetes) and 15 patients with benign liver disease without DM. There were no significant differences in age and sex distribution between the 2 groups. The alanine aminotransferase (ALT) levels of the 2 groups were analyzed at 1, 3, and 5 days after resection (Supporting Table 2). Informed consent was obtained from all participants, and the study was approved by the local ethics committee of Nanjing Medical University, Nanjing, China.

ANIMALS

Male WT C57BL/6 mice (6-8 weeks old) were purchased from the Animal Resources of Nanjing Medical University. Animals were housed under specific pathogen-free conditions and received humane care according to a protocol approved by the Institutional Animal Care and Use Committee of Nanjing Medical University.

MOUSE DIABETES AND LIVER IRI MODEL

Streptozotocin (STZ; 40 mg/kg) or vehicle control (sodium citrate buffer) was injected intraperitoneally (IP) into separate groups of 6-week-old mice for 5 consecutive days. Mice were anesthetized, and an atraumatic clip was used to interrupt the arterial and portal venous blood supply to the cephalad liver lobes for 90 minutes, as described previously.⁽²³⁾ The S1PR3 antagonist, CAY10444 (1 mg/kg, IP; Cayman Chemical, Ann Arbor, MI), was administered 30 minutes prior to ischemia.

mellitus; DMEM, Dulbecco's modified Eagle's medium; ELISA, enzyme-linked immunosorbent assay; FBS, fetal bovine serum; HG, high-glucose; HPF, high-power field; HPRT, hypoxanthine-guanine phosphoribosyltransferase; IL, interleukin; IP, intraperitoneally; IR, ischemia/reperfusion; IRI, ischemia/reperfusion injury; KC, Kupffer cell; LG, low-glucose; LPS, lipopolysaccharide; MRC1, mannose receptor C-type 1; NOS2, nitric oxide synthase 2; NS, nonspecific; p-STAT, phosphorylated signal transducer and activator of transcription; RT-PCR, real-time polymerase chain reaction; S1P, sphingosine-1-phosphate; S1PR, sphingosine-1-phosphate receptor; shRNA, short hairpin RNA; siRNA, small interfering RNA; SPHK, sphingosine kinase; STZ, streptozotocin; T1D, type 1 diabetes; T2D, type 2 diabetes; TNF- α , tumor necrosis factor α ; WT, wild-type.

Address reprint requests to Xuebao Wang, M.D., Hepatobiliary Center, The First Affiliated Hospital of Nanjing Medical University, Key Laboratory of Liver Transplantation, Chinese Academy of Medical Sciences, Nanjing 210029, China. Telephone: +1-86-025-83718836; FAX: +1-86-025-84670769; E-mail: wangxb@njmu.edu.cn;

Additional supporting information may be found in the online version of this article.

**These authors contributed equally to this work.*

This study was supported by the Foundation of Jiangsu Collaborative Innovation Center of Biomedical Functional Materials, the Priority Academic Program Development of Jiangsu Higher Education Institutions, and the National Natural Science Foundation of China (81400650, 814700901, 81273261, and 81270583).

Copyright © 2019 The Authors. Liver Transplantation published by Wiley Periodicals Inc., on behalf of the American Association for the Study of Liver Diseases. This is an open access article under the terms of the Creative Commons Attribution-NonCommercial License, which permits use, distribution, and reproduction in any medium, provided the original work is properly cited and is not used for commercial purposes.

View this article online at wileyonlinelibrary.com.

DOI 10.1002/lt.25470

Potential conflict of interest: Nothing to report.

SERUM BIOCHEMICAL MEASUREMENTS AND LIVER HISTOPATHOLOGY

Serum ALT and aspartate aminotransferase (AST) levels were measured with an AU5400 automated chemical analyzer (Olympus, Tokyo, Japan). Liver sections were stained with hematoxylin-eosin. Liver macrophages and neutrophils were detected using primary rat anti-mouse CD68 mitochondrial antibody (Abcam, Cambridge, United Kingdom) and Ly6G mitochondrial antibody (Abcam), respectively.

IMMUNOFLUORESCENCE STAINING OF LIVER SECTIONS

Immunofluorescence staining of optimal cutting temperature sections was performed by 1% Triton X-100, followed by incubation with rabbit anti-S1PR3 (1:100; ImmunoWay, Plano, TX), rabbit anti-CD86 (1:100; Abcam), rabbit anti-CD206 (1:100; Abcam), and rat anti-CD68 (1:100; Abcam) overnight at 4°C.

ASSAY OF S1P

Liver tissue was homogenized or macrophages were sonicated in ice-cold 50 mM of Tris buffer (pH 7.4) containing 0.25 M of sucrose, 25 mM of KCl, 0.5 mM of ethylene diamine tetraacetic acid, and 1% phosphatase inhibitor cocktail (Sigma-Aldrich, St. Louis, MO). S1P in supernatants was determined using an enzyme-linked immunosorbent assay (ELISA) kit (Echelon Inc., Salt Lake City, UT).

CELL CULTURE

Bone marrow-derived macrophages (BMDMs) were isolated and cultured in low-glucose (LG; 5 mM) or high-glucose (HG; 30 mM) Dulbecco's modified Eagle's medium (DMEM) with 10% fetal bovine serum (FBS), 10% L929 conditioned medium, 100 U/mL of penicillin, and 100 mg/mL of streptomycin for 6 days. At day 7, macrophages were stimulated with lipopolysaccharide (LPS; 1 µg/mL; Sigma-Aldrich) for 0–24 hours.

Primary liver Kupffer cells (KCs) were isolated from the C57BL/6 WT mice as follows. Mouse livers were perfused in situ via the portal vein with Hank's balanced salt solution, followed by 0.27% collagenase IV (Sigma-Aldrich). Perfused livers were then dissected and pressed through 70-µm cell strainers, followed by suspension in 40 mL of DMEM supplemented with 10% FBS.

Nonparenchymal cells were separated from hepatocytes by centrifugation at 50g for 2 minutes 3 times. The adherent cells (KCs, 80%–90% F4/80 positive) were used for further in vivo experiments.

S1PR3 KNOCKDOWN WITH SMALL INTERFERING RNA

The small interfering RNA (siRNA) sequence against mouse S1PR3 was generated by Genepharma (Shanghai, China) with the target sequence 5'-CCAA-GCAGAAGUAAGUCAATT-3'. The nonspecific (NS) siRNA sequence 5'-UUCUCCGAACGUGUCAC-GUTT-3' served as a control. In total, 10⁶ BMDMs/well were transfected in vitro with mouse S1PR3-specific siRNAs, or nonspecific siRNA (Genepharma) using Lipofectamine 3000 reagent (Invitrogen, San Diego, CA).

LENTIVIRAL VECTOR CONSTRUCTION AND TRANSDUCTION OF BMDMS

Plasmid vectors expressing short hairpin RNAs (shRNAs) were constructed using the pLV3-S1PR3-shRNA vector (Genepharma). For lentiviral transduction, 10⁶ cells/well were seeded in 6-well tissue culture plates and infected the following day with lentiviruses.

TOTAL BODY IRRADIATION AND CELL TREATMENT

Mice received total body irradiation with a total dose of 5 Gy per animal using an X-ray generator (Rad Source RS2000 irradiator, Rad Source Technologies, Coral Springs, USA). BMDMs cultured under HG conditions were transfected with a lentivirus-mediated S1PR3 slicing vector or control vector. Cells (2 × 10⁶) from different treatment groups were injected via the tail vein into the myeloid-destructive mice before IR.

QUANTITATIVE REAL-TIME POLYMERASE CHAIN REACTION

Quantitative real-time polymerase chain reaction (qRT-PCR) was performed using a 7900 Real-Time PCR System (Applied Biosystems, Foster City, CA) with Fast Start Universal SYBR Green Master Mix (Takara, Osaka, Japan). The primer sequences are shown in Supporting Table 1.

WESTERN BLOTTING

Tissue or cellular proteins were extracted and subjected to 10% sodium dodecyl sulfate–polyacrylamide gel electrophoresis and transferred to polyvinylidene difluoride membranes (Bio-Rad, Hercules, CA). Rabbit anti-S1P, S1PR3, phosphorylated signal transducer and activator of transcription (p-STAT) 1, p-STAT3, p-STAT6, STAT1, STAT3, and STAT6 (Abcam) and β -actin (Cell Signaling Technology, Danvers, MA) were used.

ENZYME-LINKED IMMUNOSORBENT ASSAY

Secretion of cytokines tumor necrosis factor α (TNF- α), interleukin (IL) 6, and IL10 in cell culture supernatants or serum was measured by ELISA (eBioscience, San Diego, CA).

STATISTICAL ANALYSIS

The results are presented as the mean \pm standard deviation. Multiple group comparisons were performed using 1-way analysis of variance followed by Bonferroni's post hoc test. Statistical analysis was performed using SPSS, version 22.0 (SPSS Inc., Chicago, IL) and unpaired Student *t* tests. A *P* value < 0.05 indicated statistical significance.

Results

ACTIVATION OF THE S1P/S1PR3 PATHWAY IN LIVER TISSUE AND KCS FROM PATIENTS WITH DM

Human liver tissues were collected from 15 patients with DM and 15 healthy controls (Supporting Table 2). We first examined the gene expression of sphingosine kinase (SPHK) 1 and SPHK2, which represented S1P biosynthesis. mRNA expression of SPHK1 and SPHK2 were significantly up-regulated compared with the normal controls (Fig. 1A). Quantitative RT-PCR also showed that patients with DM had elevated levels of S1PR3 but not S1PR1 or S1PR2 (Fig. 1B). Consistent with the mRNA expression levels of S1P biosynthesis, the tissue levels of S1P were also significantly increased in patients with DM compared with healthy controls (Fig. 1C). Western blot also showed the increased levels of S1PR3 in patients with DM (Fig. 1D). To

determine whether S1PR3 was activated in the macrophages in response to in vivo hyperglycemia, we performed immunofluorescent staining for CD68 and S1PR3. Results showed that S1PR3 colocalized in macrophages (KCs), and S1PR3-positive macrophages were significantly increased in patients with DM compared with normal controls (Fig. 1E,F). Thus, "specifically" means that the S1P/S1PR3 pathway is activated in only the S1P/S1PR₁₋₃ system, not S1P/S1PR1 or S1P/S1PR2. These data indicate that hyperglycemia triggered the S1P/S1PR3 pathway in liver tissues and KCs from patients with DM.

ACTIVATION OF THE S1P/S1PR3 PATHWAY IN LIVER TISSUE AND KCS FROM DIABETIC MICE

We injected WT C57BL/6 mice with multiple injections of low-dose STZ prior to the start of liver IRI. Hyperglycemia was confirmed at day 14, and then a sham or IR procedure was performed in diabetic (STZ) and control mice. There was no effect of STZ on liver S1P/S1PR levels before hyperglycemia was established in mice. To determine whether the S1P/S1PR3 signaling pathway was activated in diabetic mice, we harvested liver tissue from diabetic and control mice. Quantitative RT-PCR showed that mRNA expression of SPHK1 and SPHK2 were both significantly increased in diabetic mice (Fig. 2A,B). Consistent with these results, the tissue levels of S1P were also increased in diabetic mice compared with the controls (Fig. 2C). The mRNA levels of S1PR3 were significantly increased in diabetic mice, whereas S1PR1 and S1PR2 were not (Fig. 2D-F). Western blot results further confirmed the higher expression of S1PR3 in diabetic mice (Fig. 2G). More importantly, dual immunofluorescence staining of CD68 and S1PR3 demonstrated that S1PR3 colocalized in macrophages (KCs) and S1PR3-positive macrophages were significantly increased in STZ-induced diabetic mice compared with controls (Fig. 2H,I). Next, we evaluated expression of the hyperglycemia-activated S1P/S1PR3 pathway in liver IRI. Liver tissues were collected 6 and 24 hours after reperfusion. Compared with the control mice, mRNA expression of SPHK1, SPHK2, and S1PR3 in diabetic mice was significantly increased at 6 hours, but not at 24 hours, after reperfusion (Fig. 2A,B,F). Consistent with mRNA expression levels, the tissue levels of S1P and S1PR3 in diabetic mice were also significantly increased after 6 hours of reperfusion (Fig. 2C,G). These results indicate that hyperglycemia triggered the S1P/S1PR3

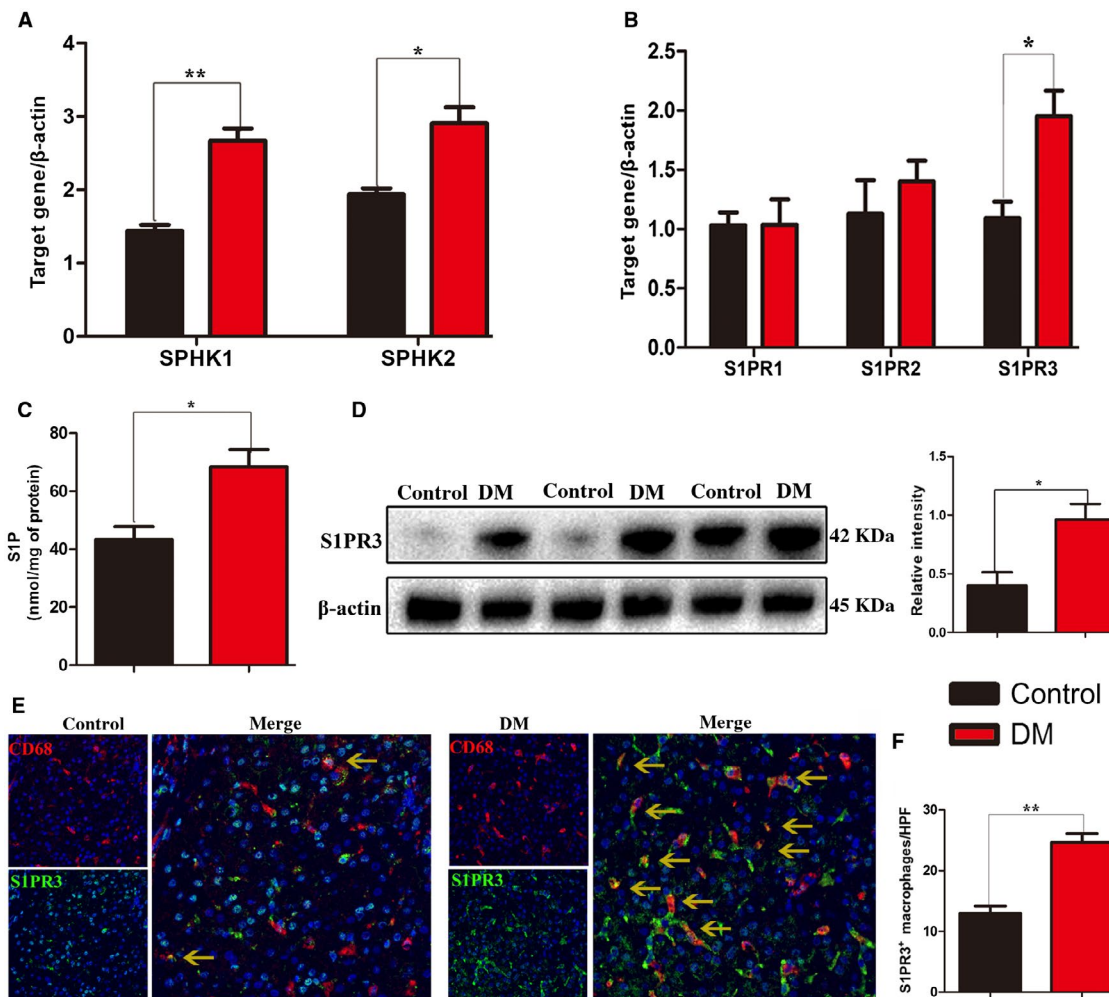


FIG. 1. S1P/S1PR3 pathway is activated in liver tissue and KCs from patients with DM. The DM group represented patients with benign liver disease with diabetes; the control group represented patients with benign liver disease without diabetes. (A) The mRNA levels of SPHK1 and SPHK2 in liver tissues of patients with DM and normal controls. (B) The mRNA levels of S1PR1, S1PR2, and S1PR3 in liver tissues of patients with DM and normal controls. (C) S1P was quantified by ELISA in liver tissues of patients with DM and normal controls. (D) A Western blot analyses of S1PR3 in patients with DM and normal controls are shown and relative density ratios of S1PR3 in different groups are also shown. (E) Dual immunofluorescence staining of CD68 (red) and S1PR3 (green). DAPI was used to visualize nuclei (blue). (F) S1PR3⁺ macrophages were quantitated by counting the number of positive cells/area. These are representative results of 3 independent experiments. **P* ≤ 0.05; ***P* ≤ 0.01.

pathway in liver tissues and KCs from diabetic mice and that it was also involved in liver IRI.

NECESSITY OF THE S1P/S1PR3 PATHWAY FOR HYPERGLYCEMIA-EXACERBATED LIVER IRI

According to the expression of S1P and S1PR3 in diabetic and control mice at different times after

reperfusion, we established a 6-hour-reperfusion IR model to further explore the role of the hyperglycemia-activated S1P/S1PR3 pathway in liver IRI. Diabetic mice developed much more severe liver injury after 90 minutes of ischemia and 6 hours of reperfusion, as demonstrated by significantly increased levels of serum ALT and AST and more severely damaged liver architecture with higher Suzuki scores compared with the controls (Fig. 3A-D). We then

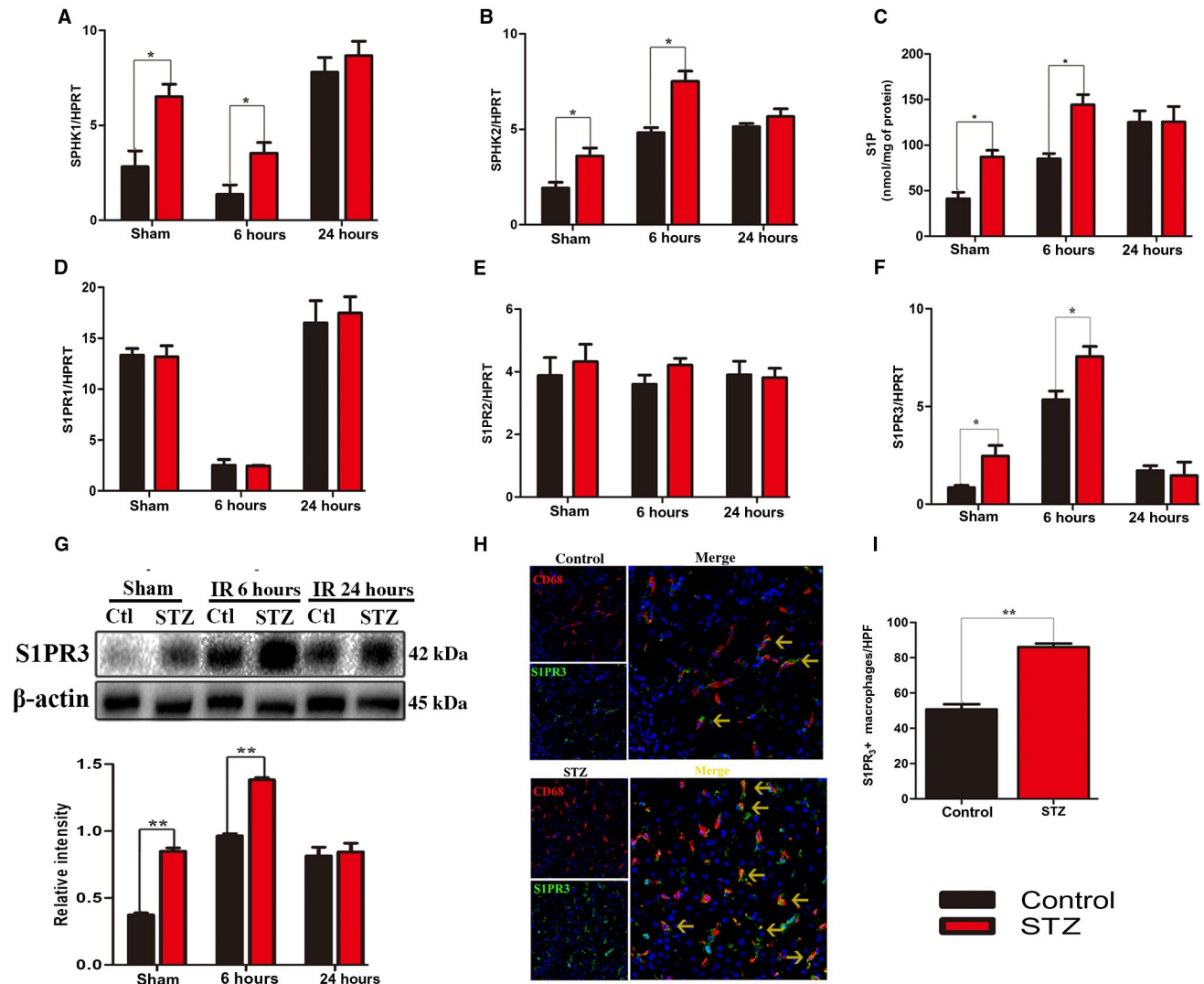


FIG. 2. S1P/S1PR3 pathway is activated in liver tissue and KCs from diabetic mice. Diabetic (STZ) and control mice were prepared and subjected to a sham or IR procedure. Liver tissues in different groups were collected. The mRNA levels of (A) SPHK1 and (B) SPHK2 in liver tissues of different groups were determined by quantitative RT-PCR. (C) S1P in liver tissues of different groups were quantified by ELISA. The mRNA levels of (D) S1PR1, (E) S1PR2, and (F) S1PR3 in liver tissues of different groups are shown. (G) S1PR3 protein expression in liver tissues was measured by Western blotting. Relative density ratios of target proteins in different groups are shown. (H) Dual immunofluorescence staining of CD68 (red), S1PR3 (green), and DAPI (blue) in diabetic (STZ) and control mice. (I) S1PR3⁺ macrophages were quantified by counting the number of positive cells/area as shown in G. These are representative results of 3 independent experiments: n = 5 or 6 mice/group. * $P \leq 0.05$; ** $P \leq 0.01$.

administered a single dose of S1PR3 inhibitor CAY10444 prior to the start of liver IRI. We found that CAY10444 alleviated liver IRI only in diabetic but not control mice, as measured by serum ALT and AST and liver histology (Fig. 3A-D). These data demonstrated that the S1P/S1PR3 pathway played a key role in hyperglycemia-exacerbated liver IRI.

NECESSITY OF THE S1P/S1PR3 PATHWAY FOR HYPERGLYCEMIA-ENHANCED INFLAMMATION AFTER IR

Inflammation is an important factor in liver IRI. To determine if the S1P/S1PR3 pathway regulated hyperglycemia-aggravated proinflammatory responses

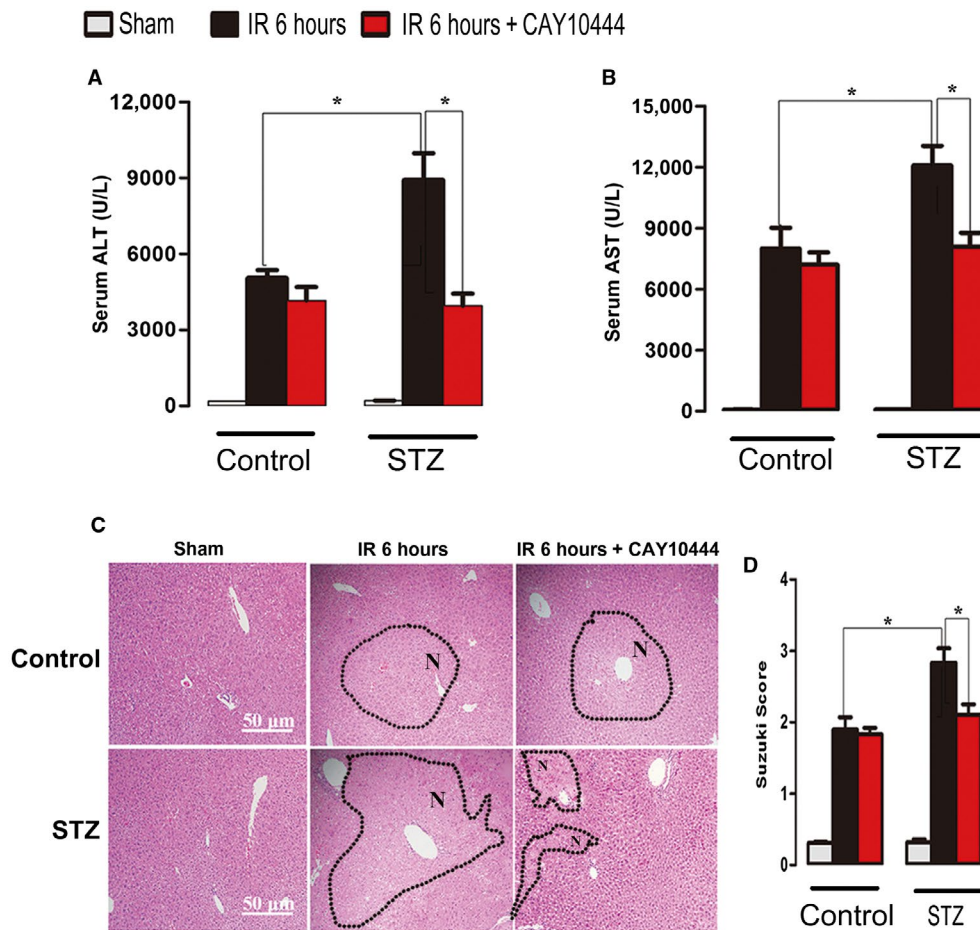


FIG. 3. The S1P/S1PR3 pathway is critical for hyperglycemia-exacerbated liver IRI. Diabetic (STZ) and control mice were prepared. The S1PR3 antagonist CAY10444 was administered 30 minutes prior to ischemia and then the IR or sham procedure was performed. At 6 hours after reperfusion, liver tissues and serum samples were collected. Serum (A) ALT and (B) AST levels of mice with different treatments are shown. (C) Representative liver histological (hematoxylin-eosin staining) and (D) average Suzuki scores of mice with different treatments are given. These are representative results of 3 independent experiments: $n = 5$ or 6 mice/group, $*P \leq 0.05$; $**P \leq 0.01$.

during IR, we analyzed expression of inflammatory cytokines TNF- α , IL6, and IL10 in untreated and CAY10444-treated diabetic mice as well as in controls. As expected, compared with the controls, diabetic mice had significantly increased expression of TNF- α and IL6 and attenuated expression of IL10 at both the gene and protein levels after IR (Fig. 4A,B). More importantly, CAY10444 significantly inhibited hyperglycemia-enhanced expression of TNF- α and IL6 but increased hyperglycemia-decreased expression of IL10 in diabetic mice at both the gene and protein levels after IR (Fig. 4A,B). We

also evaluated if the hyperglycemia-activated S1P/S1PR3 pathway affected macrophage and neutrophil functions in ischemic liver tissues. We found that CD68 $^{+}$ macrophages and Ly6G $^{+}$ neutrophils were both significantly increased in diabetic mice compared with the controls after IR (Fig. 4C-F). CD68 $^{+}$ macrophages and Ly6G $^{+}$ neutrophils were markedly lower in CAY10444-treated diabetic mice compared with untreated diabetic mice after IR (Fig. 4C-F). These results indicate that the S1P/S1PR3 pathway is essential for hyperglycemia-promoted proinflammatory responses in liver IRI.

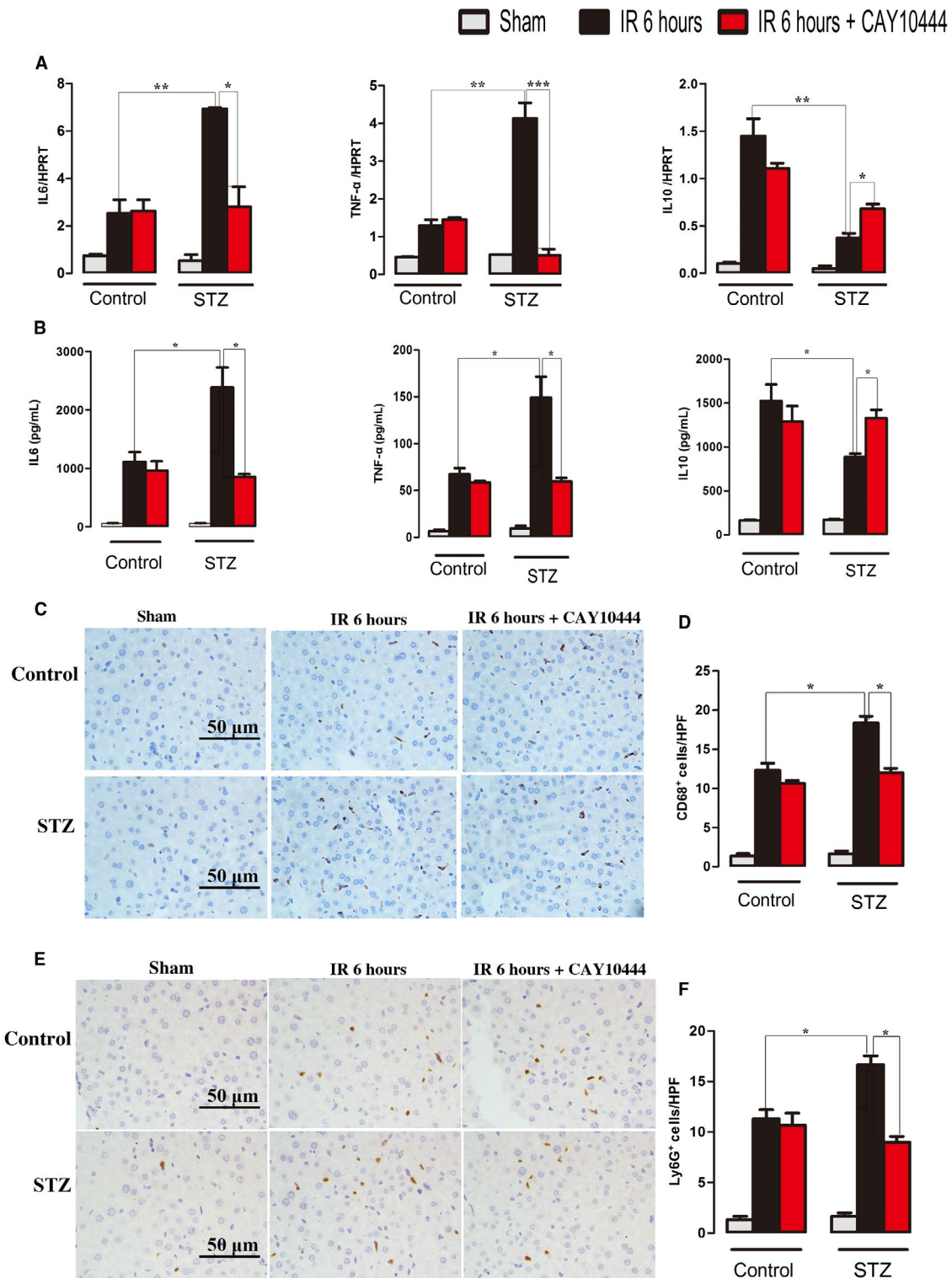


FIG. 4. The S1P/S1PR3 pathway is essential for hyperglycemia-enhanced inflammation after IR. (A) Inflammatory gene expression in liver tissues of mice with different treatments was evaluated by quantitative RT-PCR. (B) Serum levels of inflammatory cytokines were measured by ELISA. (C) Macrophage and (E) neutrophil infiltration were analyzed by immunohistological staining with antibodies against CD68 and Ly6G, respectively (original magnification $\times 40$). (D) CD68⁺ or (F) Ly6G⁺ cells were quantitated by counting the number of positive cells/area as shown in C and E. These are representative results of 3 independent experiments: $n = 5$ or 6 mice/group, * $P \leq 0.05$; ** $P \leq 0.01$; *** $P \leq 0.001$.

INVOLVEMENT OF M1/M2 POLARIZATION IN HYPERGLYCEMIA-TRIGGERED S1P/S1PR3 PATHWAY IN LIVER IRI

To investigate whether hyperglycemia-exacerbated liver IRI influenced macrophage polarization, we measured expression of macrophage polarization markers in the liver by quantitative RT-PCR. Compared with the controls, diabetic mice expressed constitutively higher levels of nitric oxide synthase 2 (NOS2), CD80, and CD86 (M1 marker) but lower levels of arginase 1 (ARG1), mannose receptor C-type 1 (MRC1), and CD163 (M2 marker) in both the sham and IR (6 hours of reperfusion) groups (Fig. 5A-F). More importantly, the S1PR3 antagonist CAY10444 could reverse hyperglycemia-modulated M1/M2 polarization both before and after IRI (Fig. 5A-F). Western blotting also showed that diabetic mice had enhanced activation (phosphorylation) of STAT1 but reduced activation of STAT3 and STAT6 in the sham and IR groups (Fig. 5G,H). CAY10444-treated diabetic mice had reduced activation (phosphorylation) of STAT1 but increased activation of STAT3 and STAT6 in the sham and IR groups (Fig. 5G,H). We then marked M1 macrophages with CD86 and M2 macrophages with CD206 in IR liver tissue. Compared with control mice subjected to IR, dual immunofluorescence staining showed that CD86-positive macrophages were significantly increased and CD206-positive macrophages were significantly decreased in diabetic mice subjected to IR. CAY10444 decreased CD86-positive macrophages and increased CD206-positive macrophages in the livers of diabetic mice subjected to IR (Fig. 5I-L). These results suggest that the hyperglycemia-triggered S1P/S1PR3 pathway regulates M1/M2 polarization in liver IRI.

M1/M2 POLARIZATION INVOLVEMENT IN HG-MEDIATED INFLAMMATORY RESPONSES IN MACROPHAGES

To explore whether M1/M2 polarization is involved in HG-mediated inflammatory responses in macrophages *in vitro*, we differentiated BMDMs in LG (5 mM) or HG (30 mM) conditions for 7 days and stimulated them with LPS for 24 hours. We measured the gene expression of M1/M2 polarization markers in macrophages by quantitative RT-PCR. Consistent

with the *in vivo* results, HG-BMDMs expressed higher levels of NOS2 but lower levels of ARG1 and MRC1 compared with LG-BMDMs, as well as after LPS stimulation (Fig. 6A). Compared with the LG-BMDMs, significantly higher levels of proinflammatory TNF- α and IL6 gene expression, but lower levels of anti-inflammatory IL10 gene expression, were induced in HG-BMDMs after LPS stimulation (Fig. 6B). Consistent with the genetic data, ELISA results also showed that HG-BMDMs produced significantly higher levels of proinflammatory TNF- α (at 6 and 24 hours) and IL6 (at 6, 12, and 24 hours), but lower levels of IL10 (at 6 hours), compared with LG-BMDMs after LPS stimulation (Fig. 6C). Given that *in vivo* hyperglycemia activated S1P/S1PR3 in liver IRI, we determined if HG concentration had similar effects in macrophages *in vitro*. Consistent with the *in vivo* results, HG concentration triggered higher mRNA of SPHK1, SPHK2, and S1PR3 in BMDMs (Fig. 6D). More importantly, ELISA and Western blot results further confirmed the higher levels of S1P and S1PR3 in BMDMs under HG concentration (Fig. 6E,F). In addition, BMDMs under HG concentration with LPS stimulation also had elevated levels of S1P and S1PR3 compared with BMDMs under LG concentration with LPS stimulation (Fig. 6E,F).

NECESSITY OF THE S1P/S1PR3 PATHWAY FOR HG-REGULATED M1/M2 POLARIZATION IN MACROPHAGES

To further explore the role of the S1P/S1PR3 pathway in HG-regulated M1/M2 polarization in macrophages, we transfected HG-BMDMs with S1PR3-siRNA or NS-siRNA. S1PR3-siRNA reduced HG-triggered S1PR3 gene expression in macrophages (Fig. 7A). The efficacy of S1PR3-siRNA was also confirmed *in vitro* by Western blotting (Fig. 7B). These cells were stimulated with LPS for 24 hours. S1PR3-knockdown HG-BMDMs expressed constitutively higher levels of ARG1 and MRC1 but lower levels of NOS2 after LPS stimulation (Fig. 7C). S1PR3-knockdown HG-BMDMs also decreased proinflammatory gene expression of TNF- α and IL6 but increased anti-inflammatory gene expression of IL10 (Fig. 7D). Consistent with gene expression, ELISA showed that S1PR3-knockdown HG-BMDMs produced significantly lower levels of proinflammatory TNF- α (at 6, 12, and 24 hours) and IL6 (at 6 and 12 hours)

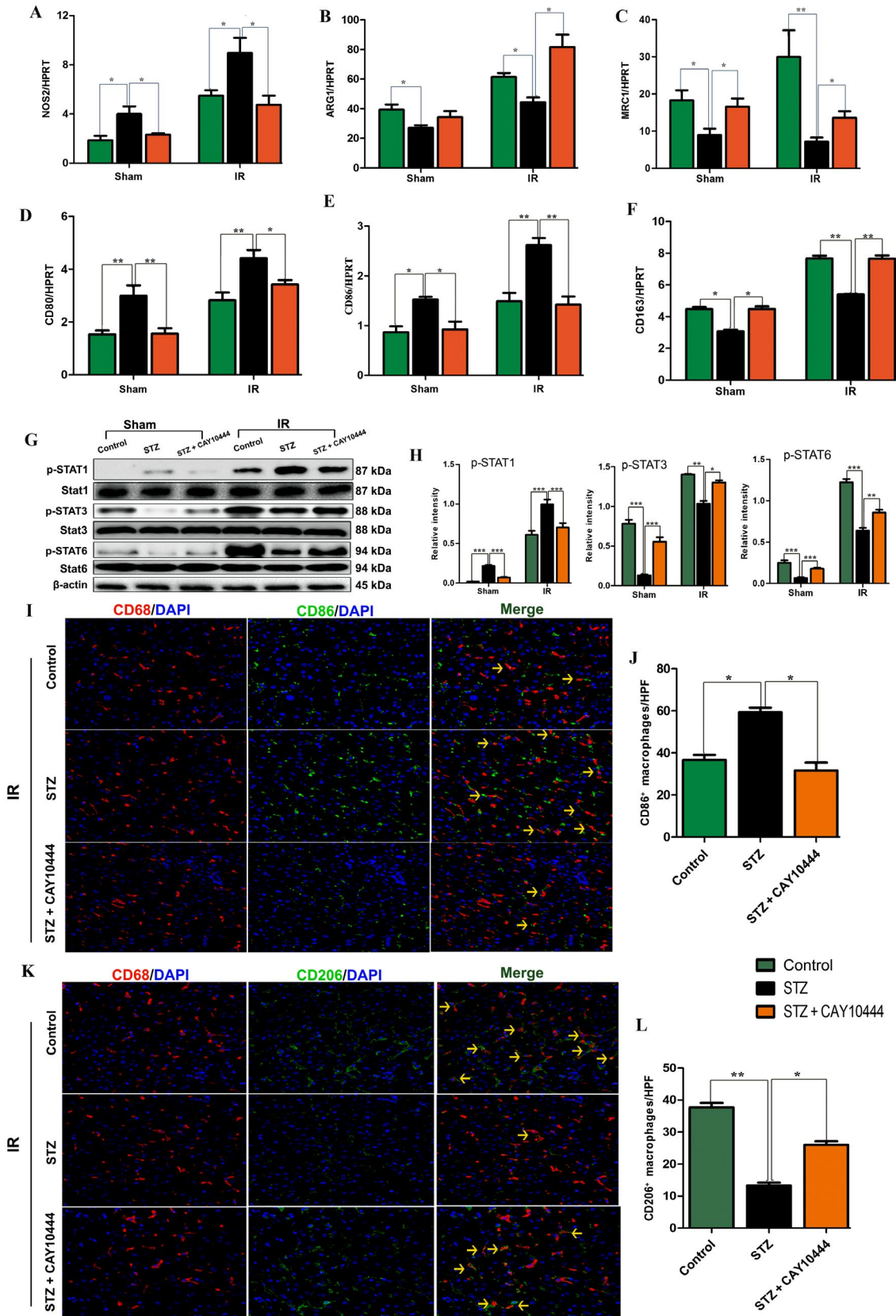


FIG. 5. M1/M2 polarization is involved in activation of the hyperglycemia-triggered S1P/S1PR3 pathway in liver IRI. Diabetic (STZ) and control mice were prepared. The S1PR3 antagonist CAY10444 was administered 30 minutes prior to ischemia and then the IR or sham procedure was performed. At 6 hours after reperfusion, liver tissues were collected. M1/M2 marker gene expression was measured by quantitative RT-PCR, including (A) NOS2, (B) ARG1, (C) MRC1, (D) CD80, (E) CD86, and (F) CD163. (G) Liver tissue levels of p-STAT1, p-STAT3, p-STAT6, and β -actin protein were analyzed by Western blotting. (H) Relative density ratios of target proteins in different groups as shown in G. (I) Dual immunofluorescence staining of CD68 (red) and CD86 (green) in the different groups after IR. (K) Dual immunofluorescence staining of CD68 (red) and CD206 (green) in the different groups after IR. DAPI was used to visualize nuclei (blue). (J) CD86⁺ macrophages and (L) CD206⁺ macrophages were quantitated by counting the number of positive cells/area as shown in F and H. These are representative results of 3 independent experiments: n = 5 or 6 mice/group. * $P \leq 0.05$; ** $P \leq 0.01$; *** $P \leq 0.001$.

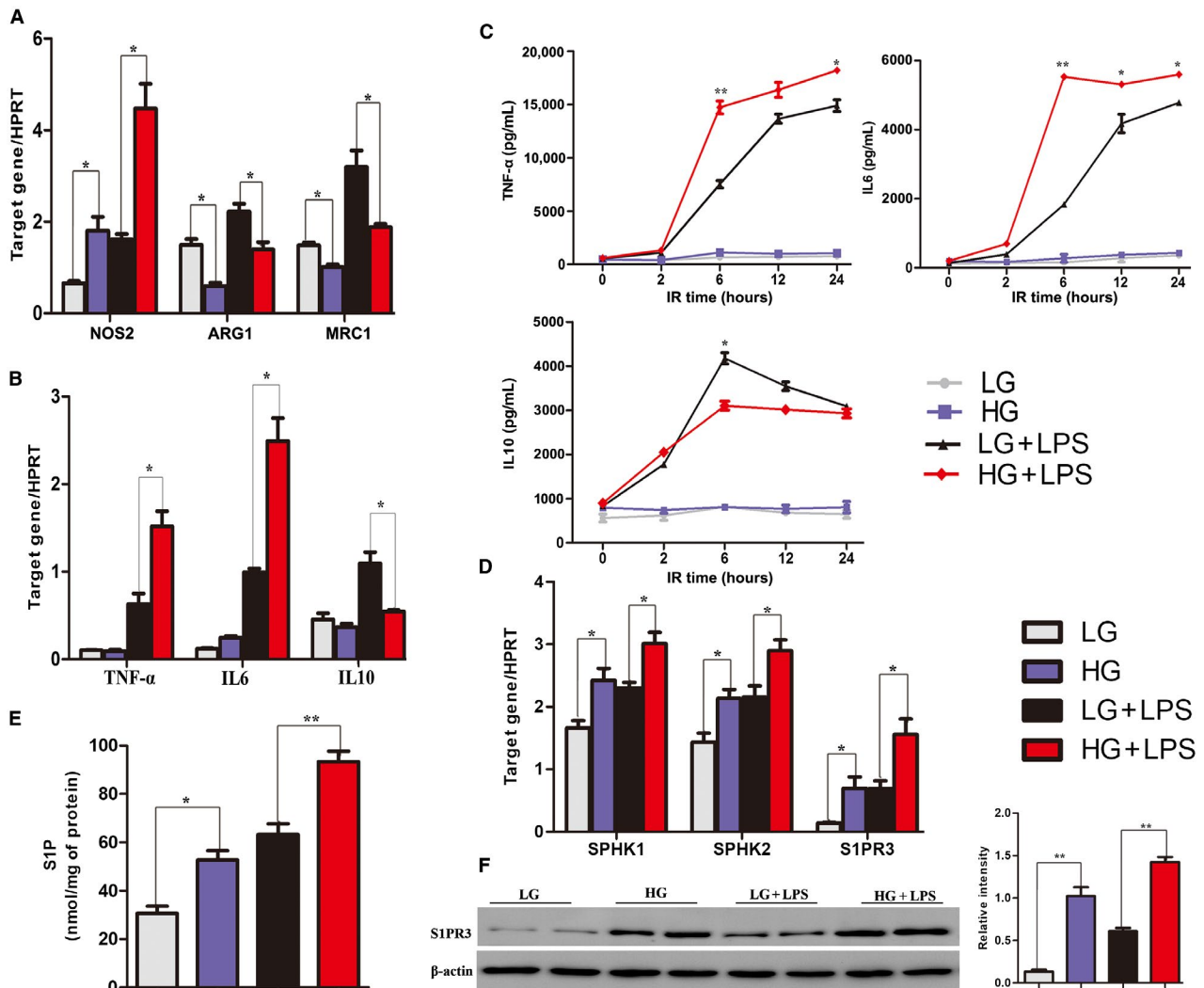


FIG. 6. M1/M2 polarization is involved in HG-mediated inflammatory responses in macrophages. BMDMs were differentiated under LG or HG conditions. These cells were then stimulated with LPS (1 μ g/mL) for 24 hours. (A) M1/M2 marker gene expression in BMDMs with different treatments was measured by quantitative RT-PCR. (B) Inflammatory gene expression in BMDMs with different treatments was measured by quantitative RT-PCR. (C) Cytokine levels in culture supernatants were measured by ELISA. (D) SPHK1, SPHK2, and S1PR3 gene expression in BMDMs with different treatments were determined by quantitative RT-PCR. (E) S1P in BMDMs were quantified by ELISA. (F) S1PR3 protein expression in BMDMs with different treatments was measured by Western blotting. Relative density ratios of target proteins in different groups were also shown. * $P \leq 0.05$; ** $P \leq 0.01$.

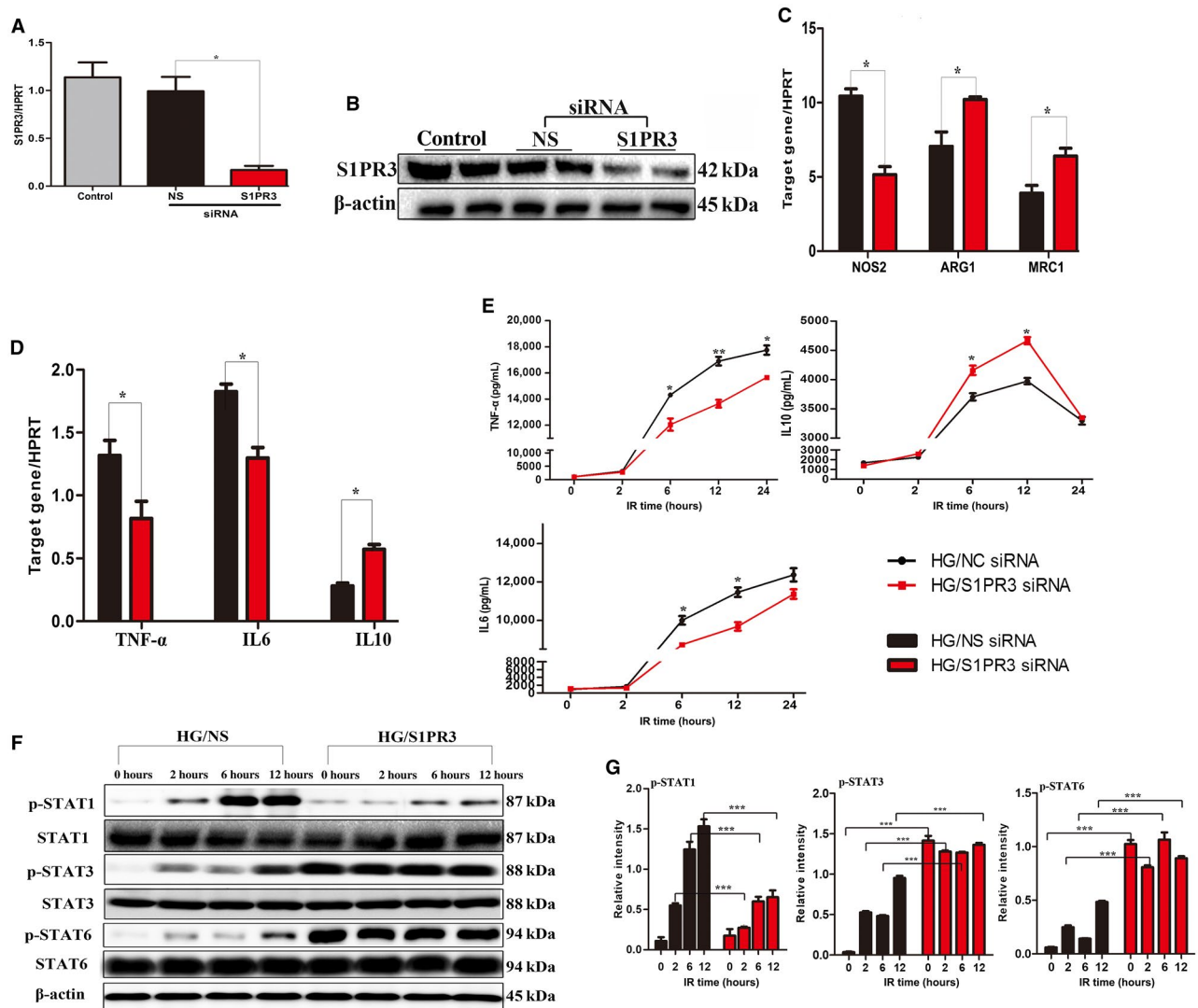


FIG. 7. The S1P/S1PR3 pathway is critical for HG-regulated M1/M2 polarization in macrophages. BMDMs were differentiated under HG conditions. NS or S1PR3-specific siRNA was transfected in vitro in HG-cultured BMDMs. S1PR3 gene and protein expression was determined by (A) quantitative RT-PCR and (B) Western blotting. These cells were then stimulated with LPS for 24 hours. (C) M1/M2 marker gene expression was measured by quantitative RT-PCR. (D) Inflammatory gene expression in BMDMs was determined by quantitative RT-PCR. (E) Cytokine levels in culture supernatants were measured by ELISA. (F) The intracellular levels of p-STAT1, p-STAT3, p-STAT6, and β -actin protein were analyzed by Western blotting. (G) Relative density ratios of target proteins in different groups as shown in F. * $P \leq 0.05$; ** $P \leq 0.01$; *** $P \leq 0.001$.

but higher levels of IL10 (at 6 hours; Fig. 7E). Moreover, compared with normal HG-BMDMs, S1PR3-knockdown HG-BMDMs reduced activation (phosphorylation) of STAT1 but increased activation of STAT3 and STAT6 after LPS stimulation (Fig. 7F,G). We also isolated primary liver KCs from the C57BL/6 WT mice. Just as in the BMDM cell experiment, we transfected HG-stimulated primary KCs with S1PR3-siRNA or NS-siRNA. The efficacy

of S1PR3-siRNA was also confirmed by quantitative RT-PCR and Western blotting in vitro (Supporting Fig. 1A,B). Consistent with the results of in vitro BMDM, S1PR3-knockdown HG-KCs expressed higher levels of ARG1 and MRC1 but lower levels of NOS2 after LPS stimulation (Supporting Fig. 1C). S1PR3-knockdown HG-BMDMs also decreased proinflammatory expression of TNF- α and IL6 but increased anti-inflammatory expression of IL10 at

both the gene and protein levels (Supporting Fig. 1D,E). Moreover, compared with normal HG-KCs, S1PR3-knockdown HG-KCs reduced activation (phosphorylation) of STAT1 but increased activation of STAT6 after LPS stimulation (Supporting Fig. 1F). These data confirmed that the S1P/S1PR3 pathway was also critical for HG-regulated M1/M2 polarization in KCs. These data indicated that the S1P/S1PR3 pathway was critical for HG-regulated M1/M2 polarization in macrophages.

ADMINISTRATION OF HG-CULTURED MACROPHAGES WORSEN LIVER IRI BY REGULATING S1PR3

Many studies have used irradiation experiments to destroy bone marrow and have combined them with BMDM injection to establish a chimeric model. As liver resident KCs are CD11b negative and relatively radiation resistant, experiments using bone marrow chimeras document functions of infiltrating macrophages but not resident macrophages.^(24,25) C57BL/6 WT mice were irradiated at 5 Gy to destroy bone marrow. The depletion of myeloid cells after total body irradiation was confirmed by checking CD45- and CD11b-positive cells using flow cytometric analysis (Supporting Fig. 2). BMDMs isolated from normal mice were cultured and differentiated in LG (5 mM) or HG (30 mM) conditions for 7 days. BMDMs cultured in HG conditions were transfected with S1PR3-shRNA vector or the S1PR3-NC vector. Then, the above treated 2×10^6 cells were injected separately via the tail vein into the myeloid-destructive mice before IR. Thus, we divided the mice into 5 groups: no cells, LG-BMDMs, HG-BMDMs, HG/S1PR3-NC BMDMs, and HG/S1PR3-shRNA BMDMs. Liver and serum tissues were harvested separately after 90 minutes of ischemia and 6 hours of reperfusion (Fig. 8A). Compared with the no cells group, serum ALT and AST levels were significantly increased in the other 4 groups (Fig. 8B,C). The LG-BMDMs group had decreased serum ALT and AST levels compared with the HG-BMDMs group. Mice injected with S1PR3-knockdown HG-BMDMs (HG/S1PR3-shRNA BMDMs) also had markedly decreased serum ALT and AST levels compared with normal control HG-BMDMs (HG/S1PR3-NC BMDMs; Fig. 8B,C). Consistent with the enzymatic indicators

of the liver, the LG-BMDM group showed alleviated liver structural injury compared with the HG-BMDM group, including decreased severity of sinus congestion and extensive necrosis. The HG/S1PR3-shRNA BMDM group also had alleviated liver structural injury, with lower Suzuki scores compared with the HG/S1PR3-NC BMDM group (Fig. 8D,E). In terms of inflammatory factors, the LG-BMDM group had significantly reduced TNF- α and IL6 but enhanced IL10 protein expression levels in serum compared with the HG-BMDM group (Fig. 8F). Mice administered HG/S1PR3-shRNA BMDMs also had reduced TNF- α and IL6 but increased IL10 protein expression compared with the HG/S1PR3-NC BMDM group (Fig. 8F).

Discussion

DM is one of the most prevalent metabolic diseases, affecting 347 million individuals worldwide.⁽²⁶⁾ Diabetes includes T1D and T2D. T1D is caused by an attack on pancreatic β cells, resulting in the destruction of pancreatic β cells and loss of insulin secretion. In our study, we used a multiple low-dose STZ-induced diabetic mice model, which is similar to the human pathophysiology of T1D and widely used for studying type 1 DM. In addition, we also enrolled patients with T1D in the study. Consistently, we found that S1P/S1PR3 is activated in both patients with T1D and STZ-induced diabetic mice, which further demonstrates the important role of S1P/S1PR3 in T1D. DM is characterized by hyperglycemia and has been shown to trigger chronic inflammation.⁽²⁷⁾ Overwhelming epidemiological and clinical data have demonstrated that patients with DM are more sensitive to IRI.⁽²⁸⁾ Diabetes and its associated hyperglycemia are involved in a variety of ischemic tissue injuries, including in the lungs, brain, kidney, and liver.⁽²⁹⁻³²⁾ The numerous functions of S1P include the regulation of cell death, proliferation, motility, differentiation, and inflammation.⁽³³⁻³⁵⁾ Most of the effects of S1P are mediated through the S1PR family, which includes the ubiquitously expressed S1PR1, S1PR2, and S1PR3 subtypes.⁽³⁶⁾ Some research has demonstrated that the S1P/S1PR₁₋₃ system plays a key role in the development of DM.⁽³⁷⁾ However, the role of the S1P/S1PR system in hyperglycemia-exacerbated liver IRI remains uncertain.

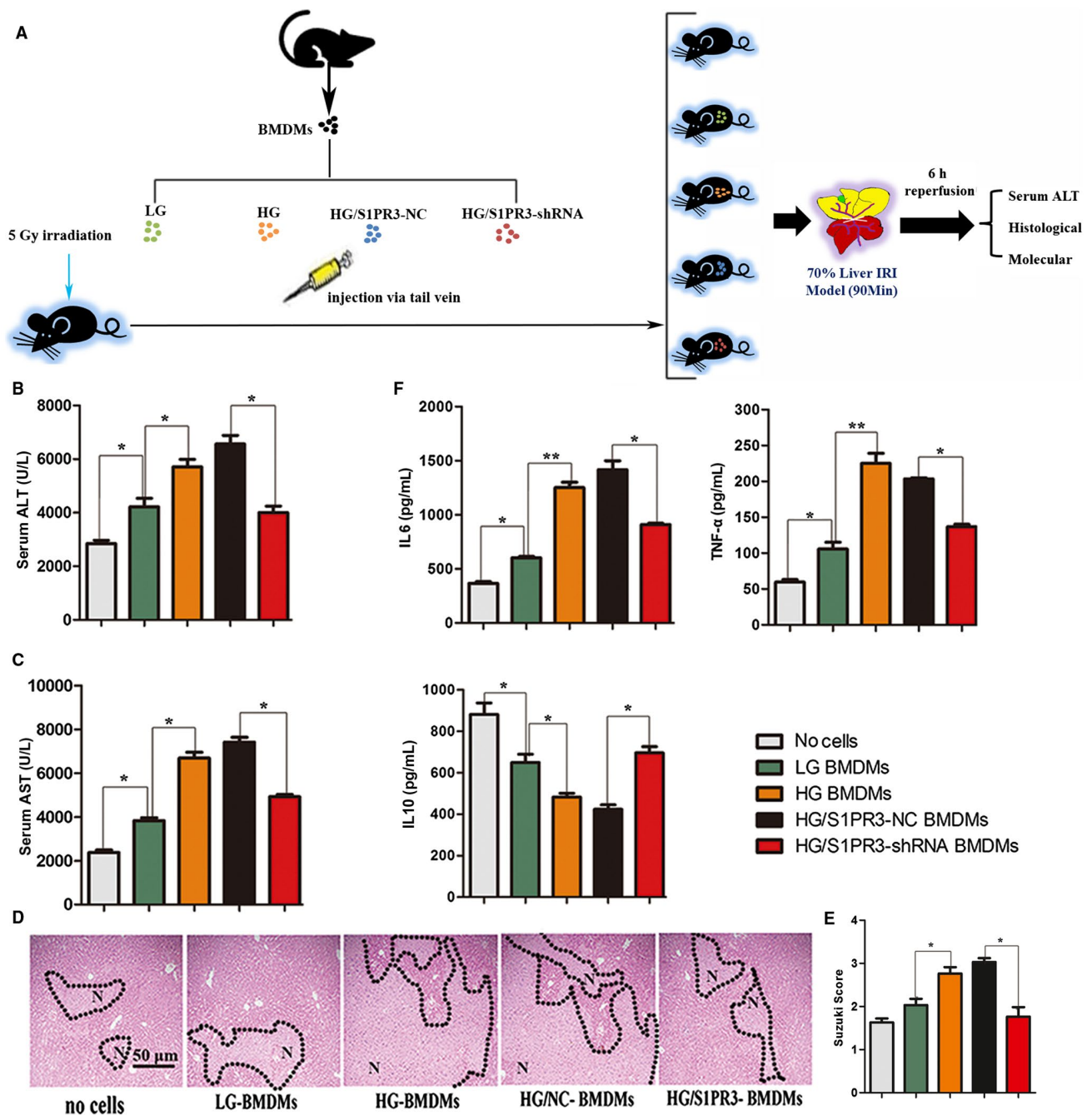


FIG. 8. Administration of HG-cultured macrophages aggravates liver IRI by regulating S1PR3. (A) C57BL/6 WT mice were irradiated at 5 Gy to destroy bone marrow. BMDMs isolated from normal mice were cultured in LG or HG medium. BMDMs cultured in HG concentration were transfected with S1PR3 knockdown or control vector. Then, the above treated 2×10^6 cells were injected separately via the tail vein into the myeloid-destructive mice before IR. Serum (B) ALT and (C) AST levels of mice with different cell treatments are shown. (D) Representative liver histology (hematoxylin-eosin staining) and (E) average Suzuki scores of mice with different cell treatments are given. (F) Serum levels of inflammatory cytokines in different groups were measured by ELISA. These are representative results of 3 independent experiments: $n = 5$ or 6 mice/group, * $P \leq 0.05$; ** $P \leq 0.01$.

S1PRs are expressed in distinct combinations in different cell types to produce biological actions, including tissue injury and repair.⁽³⁸⁾ S1PR3 activation initiates fibrosis in the heart,⁽³⁹⁾ and in mesenchymal stem cells from bone marrow, S1PR3 mediates fibrosis of the liver.^(40,41) Some research has shown that activation of S1PR3 protects the heart from IRI.^(42,43) In contrast, in some studies, S1PR3^{-/-} mice were protected from kidney IRI.⁽²⁰⁾ The roles of S1PR3 in IRI may be organ specific, which is perhaps related to cell-specific expression of S1PR3.⁽⁴⁴⁾ Previous studies have shown that DM increases susceptibility to IRI and that inflammation is an important factor in diabetes.^(31,32) In this study, we found that the S1P/S1PR3 pathway was activated in the KCs of hyperglycemic mice and that CAY10444 could suppress hepatocellular injury and inflammation after IR in STZ-treated mice but not in control mice. These findings suggest that the S1PR3 blockade attenuated hyperglycemia-exacerbated liver IRI through reducing the hyperglycemia-associated inflammation rather than by directly affecting the IRI itself.

Overall, we demonstrated that diabetes/hyperglycemia exacerbates liver IRI because of hyperinflammatory immune activation in macrophages, which is mediated by the S1P/S1PR3 pathway. The S1P/S1PR3 pathway was triggered in vivo in liver tissues from patients with DM and diabetic mice. We also found that the hyperglycemia-triggered S1P/S1PR3 pathway was involved in liver IRI. Expression of S1P and S1PR3 in diabetic mice was significantly increased after 6 hours of reperfusion. Administration of the S1PR3 antagonist CAY10444 to IR-treated diabetic mice significantly reduced liver tissue damage, decreased generation of inflammatory cytokines, and relieved inflammation. Consistent with the in vivo results, BMDMs cultured under HG conditions expressed higher levels of S1P and S1PR3 than those under LG conditions as well as after LPS treatment. Hyperglycemic BMDMs produced higher levels of TNF- α and IL6 but lower levels of IL10 after LPS stimulation. These findings establish that hyperglycemia, as a common feature of diabetes, is sufficient to activate the S1P/S1PR3 pathway in macrophages and alter their innate immune responsiveness.

Macrophages are found in all tissues and show functional diversity. They play a significant role in inflammation, homeostasis, tissue repair, and immunity.⁽⁴⁵⁾ Activated macrophages are defined as classically M1 type and, alternatively, as activated M2 type.⁽⁴⁶⁾ M1 macrophages are proinflammatory and have a central role in the host's defense against infection, whereas M2

macrophages are associated with anti-inflammatory responses.⁽⁴⁷⁾ STAT1, STAT3, and STAT6 have been reported as important regulators of macrophage polarization.⁽⁴⁸⁾ Previous studies have reported that hallmarks of diabetes, such as hyperglycemia, could induce epigenetic changes that promote an inflammatory macrophage phenotype.⁽⁴⁹⁾

In our study, M1/M2 polarization was involved in the hyperglycemia-triggered S1P/S1PR3 pathway in liver IRI. We found that the populations of KCs were not affected by S1PR3 blockade (data not published) and that only the differentiation/polarization of KCs were changed by S1PR3 blockade. Diabetic mice expressed higher gene levels of M1 macrophage markers (NOS2) but lower gene levels of M2 macrophage markers (ARG1 and MRC1), as well as after IR treatment, compared with the controls. Dual immunofluorescence staining showed that M2 macrophages in the liver of diabetic mice subjected to IR were significantly decreased, whereas those of M1 macrophages were significantly increased. Administration of CAY10444 restored M2 marker levels and M2 macrophages in the livers of diabetic mice subjected to IR.

By in vitro experiments, we confirmed that the S1P/S1PR3 pathway was critical for HG-regulated M1/M2 polarization in macrophages. We found that hyperglycemia inhibited M2-like macrophage polarization, which responded to LPS stimulation by producing lower levels of IL10, decreased M2 macrophage signature genes (ARG1 and MRC1) and reduced STAT3 and STAT6 signaling pathway activation. More importantly, we found that S1PR3 knockdown in hyperglycemic macrophages resulted in the development of M2-like macrophage polarization. We found that administration of hyperglycemic macrophages exacerbated liver IRI, whereas S1PR3-knockdown hyperglycemic macrophages reduced aggravation of liver IRI induced by hyperglycemic macrophages, which further confirmed the above results.

In summary, we demonstrated that diabetes-associated hyperglycemia has a significant negative impact on liver IRI and that the hyperglycemia-triggered S1P/S1PR3 pathway worsens liver IRI by regulating M1/M2 polarization.

REFERENCES

- 1) Groop L, Pociot F. Genetics of diabetes—are we missing the genes or the disease? *Mol Cell Endocrinol* 2014;382:726-739.

- 2) Lontchi-Yimagou E, Sobngwi E, Matsha TE, Kengne AP. Diabetes mellitus and inflammation. *Curr Diab Rep* 2013;13:435-444.
- 3) John PR, Thuluvath PJ. Outcome of liver transplantation in patients with diabetes mellitus: a case-control study. *Hepatology* 2001;34:889-895.
- 4) Shields PL, Tang H, Neuberger JM, Gunson BK, McMaster P, Pirenne J. Poor outcome in patients with diabetes mellitus undergoing liver transplantation. *Transplantation* 1999;68:530-535.
- 5) Samuelson AL, Lee M, Kamal A, Keeffe EB, Ahmed A. Diabetes mellitus increases the risk of mortality following liver transplantation independent of MELD score. *Dig Dis Sci* 2010;55:2089-2094.
- 6) Dare AJ, Plank LD, Phillips AR, Gane EJ, Harrison B, Orr D, et al. Additive effect of pretransplant obesity, diabetes, and cardiovascular risk factors on outcomes after liver transplantation. *Liver Transpl* 2014;20:281-290.
- 7) Liang T, Zhang Q, Sun W, Xin Y, Zhang Z, Tan Y, et al. Zinc treatment prevents type 1 diabetes-induced hepatic oxidative damage, endoplasmic reticulum stress, and cell death, and even prevents possible steatohepatitis in the OVE26 mouse model: important role of metallothionein. *Toxicol Lett* 2015;233:114-124.
- 8) Gill R, Tsung A, Billiar T. Linking oxidative stress to inflammation: toll-like receptors. *Free Radic Biol Med* 2010;48:1121-1132.
- 9) Schwabe RF, Brenner DA. Mechanisms of liver injury. I. TNF- α -induced liver injury: role of IKK, JNK, and ROS pathways. *Am J Physiol Gastrointest Liver Physiol* 2006;290:G583-G589.
- 10) Behrends M, Martinez-Palli G, Niemann CU, Cohen S, Ramachandran R, Hirose R. Acute hyperglycemia worsens hepatic ischemia/reperfusion injury in rats. *J Gastrointest Surg* 2010;14:528-535.
- 11) Chang N, Xiu L, Li L. Sphingosine 1-phosphate receptors negatively regulate collagen type I/III expression in human bone marrow-derived mesenchymal stem cell. *J Cell Biochem* 2014;115:359-367.
- 12) Rosen H, Stevens RC, Hanson M, Roberts E, Oldstone MB. Sphingosine-1-phosphate and its receptors: structure, signaling, and influence. *Annu Rev Biochem* 2013;82:637-662.
- 13) Orr Gandy KA, Obeid LM. Targeting the sphingosine kinase/sphingosine 1-phosphate pathway in disease: review of sphingosine kinase inhibitors. *Biochim Biophys Acta* 2013;1831:157-166.
- 14) Maceyka M, Harikumar KB, Milstien S, Spiegel S. Sphingosine-1-phosphate signaling and its role in disease. *Trends Cell Biol* 2012;22:50-60.
- 15) Liu X, Yue S, Li C, Yang L, You H, Li L. Essential roles of sphingosine 1-phosphate receptor types 1 and 3 in human hepatic stellate cells motility and activation. *J Cell Physiol* 2011;226:2370-2377.
- 16) Shi Y, Rehman H, Ramshesh VK, Schwartz J, Liu Q, Krishnasamy Y, et al. Sphingosine kinase-2 inhibition improves mitochondrial function and survival after hepatic ischemia-reperfusion. *J Hepatol* 2012;56:137-145.
- 17) Deutschman DH, Carstens JS, Klepper RL, Smith WS, Page MT, Young TR, et al. Predicting obstructive coronary artery disease with serum sphingosine-1-phosphate. *Am Heart J* 2003;146:62-68.
- 18) Bajwa A, Jo SK, Ye H, Huang L, Dondeti KR, Rosin DL, et al. Activation of sphingosine-1-phosphate 1 receptor in the proximal tubule protects against ischemia-reperfusion injury. *J Am Soc Nephrol* 2010;21:955-965.
- 19) Duan HF, Wang H, Yi J, Liu HJ, Zhang QW, Li LB, et al. Adenoviral gene transfer of sphingosine kinase 1 protects heart against ischemia/reperfusion-induced injury and attenuates its postischemic failure. *Hum Gene Ther* 2007;18:1119-1128.
- 20) Jo SK, Bajwa A, Ye H, Vergis AL, Awad AS, Kharel Y, et al. Divergent roles of sphingosine kinases in kidney ischemia-reperfusion injury. *Kidney Int* 2009;75:167-175.
- 21) Vessey DA, Kelley M, Li L, Huang Y, Zhou HZ, Zhu BQ, et al. Role of sphingosine kinase activity in protection of heart against ischemia reperfusion injury. *Med Sci Monit* 2006;12:BR318-BR324.
- 22) Ng ML, Wadham C, Sukocheva OA. The role of sphingolipid signalling in diabetes associated pathologies (Review). *Int J Mol Med* 2017;39:243-252.
- 23) Shen XD, Ke B, Zhai Y, Amersi F, Gao F, Anselmo DM, et al. CD154-CD40 T-cell costimulation pathway is required in the mechanism of hepatic ischemia/reperfusion injury, and its blockade facilitates and depends on heme oxygenase-1 mediated cytoprotection. *Transplantation* 2002;74:315-319.
- 24) Duffield JS, Forbes SJ, Constandinou CM, Clay S, Partolina M, Vuthoori S, et al. Selective depletion of macrophages reveals distinct, opposing roles during liver injury and repair. *J Clin Invest* 2005;115:56-65.
- 25) Ji H, Liu Y, Zhang Y, Shen XD, Gao F, Busuttill RW, et al. T-cell immunoglobulin and mucin domain 4 (TIM-4) signaling in innate immune-mediated liver ischemia-reperfusion injury. *Hepatology* 2014;60:2052-2064.
- 26) Danaei G, Finucane MM, Lu Y, Singh GM, Cowan MJ, Paciorek CJ, et al. National, regional, and global trends in fasting plasma glucose and diabetes prevalence since 1980: systematic analysis of health examination surveys and epidemiological studies with 370 country-years and 2.7 million participants. *Lancet* 2011;378:31-40.
- 27) Chang SC, Yang WV. Hyperglycemia, tumorigenesis, and chronic inflammation. *Crit Rev Oncol Hematol* 2016;108:146-153.
- 28) Ding M, Lei J, Han H, Li W, Qu Y, Fu E, et al. SIRT1 protects against myocardial ischemia-reperfusion injury via activating eNOS in diabetic rats. *Cardiovasc Diabetol* 2015;14:143.
- 29) Shukla V, Shakya AK, Perez-Pinzon MA, Dave KR. Cerebral ischemic damage in diabetes: an inflammatory perspective. *J Neuroinflammation* 2017;14:21.
- 30) Shen X, Hu B, Xu G, Chen F, Ma R, Zhang N, et al. Activation of Nrf2/HO-1 pathway by glycogen synthase kinase-3 β inhibition attenuates renal ischemia/reperfusion injury in diabetic rats. *Kidney Blood Press Res* 2017;42:369-378.
- 31) Yue S, Zhou HM, Zhu JJ, Rao JH, Busuttill RW, Kupiec-Weglinski JW, et al. Hyperglycemia and liver ischemia reperfusion injury: a role for the advanced glycation endproduct and its receptor pathway. *Am J Transplant* 2015;15:2877-2887.
- 32) Zhang Y, Yuan D, Yao W, Zhu Q, Liu Y, Huang F, et al. Hyperglycemia aggravates hepatic ischemia reperfusion injury by inducing chronic oxidative stress and inflammation. *Oxid Med Cell Longev* 2016;2016:3919627.
- 33) Xia P, Gamble JR, Rye KA, Wang L, Hii CS, Cockerill P, et al. Tumor necrosis factor- α induces adhesion molecule expression through the sphingosine kinase pathway. *Proc Natl Acad Sci U S A* 1998;95:14196-14201.
- 34) Olivera A, Spiegel S. Sphingosine-1-phosphate as second messenger in cell proliferation induced by PDGF and FCS mitogens. *Nature* 1993;365:557-560.
- 35) Means CK, Brown JH. Sphingosine-1-phosphate receptor signalling in the heart. *Cardiovasc Res* 2009;82:193-200.
- 36) Takuwa Y, Takuwa N, Sugimoto N. The Edg family G protein-coupled receptors for lysophospholipids: their signaling properties and biological activities. *J Biochem* 2002;131:767-771.
- 37) Shimizu H, Okajima F, Kimura T, Ohtani K, Tsuchiya T, Takahashi H, et al. Sphingosine 1-phosphate stimulates insulin

- secretion in HIT-T 15 cells and mouse islets. *Endocr J* 2000;47:261-269.
- 38) Yang L, Han Z, Tian L, Mai P, Zhang Y, Wang L, et al. Sphingosine 1-phosphate receptor 2 and 3 mediate bone marrow-derived monocyte/macrophage motility in cholestatic liver injury in mice. *Sci Rep* 2015;5:13423.
- 39) Takuwa N, Ohkura S, Takashima S, Ohtani K, Okamoto Y, Tanaka T, et al. S1P3-mediated cardiac fibrosis in sphingosine kinase 1 transgenic mice involves reactive oxygen species. *Cardiovasc Res* 2010;85:484-493.
- 40) Li C, Jiang X, Yang L, Liu X, Yue S, Li L. Involvement of sphingosine 1-phosphate (S1P)/S1P3 signaling in cholestasis-induced liver fibrosis. *Am J Pathol* 2009;175:1464-1472.
- 41) Li C, Kong Y, Wang H, Wang S, Yu H, Liu X, et al. Homing of bone marrow mesenchymal stem cells mediated by sphingosine 1-phosphate contributes to liver fibrosis. *J Hepatol* 2009;50:1174-1183.
- 42) Means CK, Xiao CY, Li Z, Zhang T, Omens JH, Ishii I, et al. Sphingosine 1-phosphate S1P2 and S1P3 receptor-mediated Akt activation protects against in vivo myocardial ischemia-reperfusion injury. *Am J Physiol Heart Circ Physiol* 2007;292:H2944-H2951.
- 43) Theilmeyer G, Schmidt C, Herrmann J, Keul P, Schafers M, Herrgott I, et al. High-density lipoproteins and their constituent, sphingosine-1-phosphate, directly protect the heart against ischemia/reperfusion injury in vivo via the S1P3 lysophospholipid receptor. *Circulation* 2006;114:1403-1409.
- 44) Bajwa A, Huang L, Ye H, Dondeti K, Song S, Rosin DL, et al. Dendritic cell sphingosine 1-phosphate receptor-3 regulates Th1-Th2 polarity in kidney ischemia-reperfusion injury. *J Immunol* 2012;189:2584-2596.
- 45) Wynn TA, Chawla A, Pollard JW. Macrophage biology in development, homeostasis and disease. *Nature* 2013;496:445-455.
- 46) Biswas SK, Mantovani A. Macrophage plasticity and interaction with lymphocyte subsets: cancer as a paradigm. *Nat Immunol* 2010;11:889-896.
- 47) Liu YC, Zou XB, Chai YF, Yao YM. Macrophage polarization in inflammatory diseases. *Int J Biol Sci* 2014;10:520-529.
- 48) Lawrence T, Natoli G. Transcriptional regulation of macrophage polarization: enabling diversity with identity. *Nat Rev Immunol* 2011;11:750-761.
- 49) Ahmed M, de Winther MPJ, Van den Bossche J. Epigenetic mechanisms of macrophage activation in type 2 diabetes. *Immunobiology* 2017;222:937-943.